

Asymptotic limits on tablet coating variability based on cap-to-band thickness distributions: a discrete element model (DEM) study

Chunlei Pei and James A. Elliott*

Department of Materials Science and Metallurgy, University of Cambridge,
27 Charles Babbage Road, Cambridge, CB3 0FS, UK

Abstract

The uniformity of the coating thickness distribution is an important quality metric in the manufacture of pharmaceutical tablets during the spray coating process. An investigation of the asymptotic limits of coating thickness variability of tablets of varying shape was carried out based on the cap-to-band coating thickness distributions. A theoretical analysis shows that the cap-to-band coating thickness ratio is expected to be equal to the cap-to-band area ratio projected onto the spray direction divided by the actual cap-to-band surface area ratio. When the cap-to-band projected area ratio is larger (or smaller) than the cap-to-band surface area ratio, the mean coating thickness on the cap is larger (or smaller) than that on the band. To verify this, the dynamics of tablets in a rotating pan was modelled using discrete element method (DEM) simulations, while an image analysis technique based on the output of DEM simulations was applied to model the spray coating process and analyse the cap-to-band coating thickness ratio. A ray-tracing sampling method was further used to obtain the cap-to-band sample ratio. It was also found that a smaller spray angle with respect to the horizontal direction can decrease and even invert the cap-to-band coating thickness ratio, leading to a larger coating thickness on the band than the cap. Nevertheless, an asymptotic value of cap-to-band relative standard deviation can be reached once the cap-to-band coating thickness ratio becomes stable during the coating process. This asymptotic limit is within the range

* * Corresponding author. Tel.: +44 1223 335987; fax: +44 1223 334567.
E-mail address: jae1001@cam.ac.uk

predicted based on the cap-to-band projected area ratio and surface area ratio.

Keywords: Discrete element method; Spray coating process; Coating thickness distribution; Cap-to-band ratio

1. Introduction

Pharmaceutical tablets are commonly spray-coated with one or more film layers for cosmetic or functional purposes (Ho *et al.*, 2007; Lin *et al.*, 2015; Sahni and Chaudhuri, 2012, Turton, 2008). The tablets are usually placed in a rotating pan, and coating material is sprayed from a nozzle onto the tablet bed inside the pan during rotation. The coating layer can be used to produce a specific colour, mask unpleasant taste and odour, or control the release of the drug. The coating thickness distribution between tablets (the “inter-tablet variability”) and within each tablet (the “intra-tablet variability”) are both crucial parameters in determining the quality of the coating process and the final tablet products (Brock *et al.*, 2013a, 2013b, Pandey *et al.*, 2006). The intra-tablet variability is of particular importance when the coating layer is used to perform specific functions during administration of the medication (Brock *et al.*, 2013b; Freireich *et al.*, 2011).

The intra-tablet variability is affected by the tablet shape and orientation distribution in the spray area (Freireich and Wassgren, 2010; Ketterhagen, 2011). Freireich and Wassgren (2010) related the evolution of the intra-tablet coating thickness distribution to the number of coating trials for spherical particles in the spray area, where a “coating trial” is defined as a visit of the tablet to the spray zone in a particular orientation for each visit. Their theoretical model was based on the change in orientation of the particle with respect to the spray direction as a function of time. In general, the intra-tablet coating variability was found to decrease with the reciprocal of the square-root of the number of visits to the spray zone. If the orientation distribution is uniformly random, the intra-particle coating variability tends asymptotically to zero with increasing number of visits.

However, if a preferred orientation exists during the process then the asymptotic value of intra-particle coating distribution will be non-zero. In reality, pharmaceutical tablets are usually irregular in shape. Ketterhagen (2011) modelled the motion and orientation of several different pharmaceutical tablet shapes in a coating pan using discrete element method (DEM) simulations. The irregular shapes of tablets were modelled by the multi-sphere (or glued-sphere) method (Kodam *et al.*, 2009) in DEM. An orientation index (OI) was introduced for the tablets, defined as the difference of standard deviations of geodesic distributions of the major axis of tablets between uniform and preferred orientations. A larger OI indicates a larger orientation preference, which implies a greater asymptotic intra-tablet coating thickness variability. Specifically, for axisymmetric tablets with a circumferential band, it leads to greater coating thickness on the cap than the band of the tablets. It was found that the pan rotation speed and pan loading have a relatively small influence on the intra-tablet coating variability, but small sphericities and larger aspect ratios can result in a larger OI.

In experimental investigations, the cap-to-band coating thickness ratio has attracted further attention, especially when the shape of the tablet is axisymmetric (Brock *et al.*, 2013b; Ketterhagen, 2011; Pérez-Ramos, 2007). Brock *et al.* (2013b) evaluated the intra-tablet coating uniformity in an active pan coating process using Terahertz Pulsed Imaging (TPI). It was found that the cap-to-band (face-to-centre) thickness ratio is generally larger than one, which means that the cap of the tablet tends to accumulate more coating material than the band. Malaterre *et al.* (2010) found a similar cap-to-band thickness ratio for a 10% coating weight gain. The authors attributed this to a longer exposure time of the tablet cap during the tablet rolling in the spray area. However, for a 18% coating weight gain, the average coating thickness on the band was slightly larger than that on the cap. Brock *et al.* (2013b) further suggested that, similarly to Ketterhagen's study (2011), the process parameters, *e.g.* the pan speed, loading and run duration, may have little effect on the cap-to-band coating thickness ratio. Pérez-Ramos (2007) defined an orientation index as the ratio of the band-to-

cap area exposed in a video analysis using biconvex tablets with black painted caps and white bands, to the actual band-to-cap surface area. An orientation index of one implies that the intra-tablet coating distribution will be uniform since all surfaces have the same probability to be exposed in the spray zone. It was found that the orientation index was generally smaller than one, indicating that the cap area is preferentially exposed. This study concluded that the tablets in the coating pan, especially those at the top free surface of the tablet bed, have a preferred orientation.

A similar image analysis method was developed further by Freireich *et al.* (2015) and applied to analyse the spray coating process based on the positions and orientations of tablets exported from DEM simulations. The surface of the tablet was meshed into triangular elements (panels) which were indexed by specified colours. Then coloured triangular elements were shown in an image and these colours were used to retrieve the information of corresponding triangular elements and identify whether these triangular elements were in the specified spray area. This method can consider the shadowing effect, in which the surface of a tablet blocked by other tablets with respect to the spray direction will be invisible on the image and remain uncoated. It was demonstrated that the orientation preference of tablets in the rotating pan resulted in a non-zero asymptotic value of the intra-tablet variability. In addition, due to the consideration of the shadowing effect, this image method can predict the asymptotic value better than the method which only considers the orientation of tablets without the shadowing effects (Freireich *et al.*, 2011).

The cap-to-band coating thickness ratio is of great importance for the spray coating process. Fundamentally, it is related with the orientation of tablets which can be observed as the cap-to-band projected area ratio with respect to the spray direction. Previous research (Pérez-Ramos, 2007; Kandela *et al.*, 2010) has suggested the relationship between these two ratios in experimental studies. In this study, we propose a mathematical analysis discussing the relationship between the cap-to-band coating thickness ratio and the orientation properties of tablets in the rotating pan in Section 2. To

verify this analysis, DEM simulations have been implemented for the dynamic behaviours of tablets in a rotating drum. Then, the spray coating process is applied to tablets based on the image analysis algorithm developed by Freireich *et al.*(2015). A ray-tracing method (Toschkoff *et al.*, 2013; Toschkoff *et al.*, 2015) is also implemented to obtain the cap-to-band sample ratio to analyse the probability of cap and band faces intersecting with the spray during the drum rotation. We show that the cap-to-band coating thickness distribution can influence the intra-tablet variability. The asymptotic limits of intra-tablet variability, which is defined as relative standard deviation (RSD) of the coating thickness distribution, are derived mathematically from cap-to-band ratios and verified by the modelling data.

2. Theoretical analysis of tablet coating thickness variation

2.1 Cap-to-band thickness ratios

In the spray coating process, liquid droplets comprised of the coating materials are sprayed onto the tablet bed. If the spray area covered by liquid droplets is assumed to be an area with uniformly distributed pixels (see Section 3.2), then in the spray zone, A , the area per pixel is:

$$A_p = \frac{A}{n_p} \quad (1)$$

where n_p is the number of pixels in the spray area. As each pixel represents a fixed spray droplet with volume V_p , the coating thickness on the cap and band areas are:

$$\mu_c = \frac{V_c}{S_c} = \frac{n_p^c V_p}{S_c} = \frac{S_c^c V_p}{A_p S_c} \quad (2)$$

$$\mu_b = \frac{V_b}{S_b} = \frac{n_p^b V_p}{S_b} = \frac{S'_b V_p}{A_p S_b} \quad (3)$$

where V_c and V_b are the spray volume on the cap and band; S'_c and S'_b are the projected areas of the cap and band to the spray direction within the spray area; n_p^c and n_p^b are the numbers of pixels in projected areas of the cap and band; and S_c and S_b are the surface areas of the cap and band. In this method, it can be seen that the coating thickness on the cap or band is the average thickness over the respective surface area. The cap-to-band coating thickness ratio can be expressed as:

$$\frac{\mu_c}{\mu_b} = \frac{S'_c/S'_b}{S_c/S_b} \quad (4)$$

From Eq. (4), it can be seen that the cap-to-band coating thickness ratio is equal to the cap-to-band project area ratio normalised by the cap-to-band surface area ratio. In order to have the same coating thickness on cap and band areas, the cap-to-band projected area ratio should be equal to the cap-to-band surface area ratio.

If the trajectory of the spray droplet is assumed to be a ray extending from the spray nozzle to the spray area, a ray-tracing method can be further used to analyse the probability of the ray making first contact with the tablet on either the cap and band area. For this ray-tracing sampling method (see Section 3.3), considering a tablet in a fixed orientation but positioned randomly in the spray area, the probability of the ray contacting the tablet on the cap or band area on the tablet is proportional to projected areas of the cap and band as:

$$m \propto S' \quad (5)$$

Then, the cap-to-band sampling ratio is equal to the cap-to-band projected area ratio as:

$$\frac{m_c}{m_b} = \frac{S_c'}{S_b'} \quad (6)$$

And also, according to Eqs. (4) and (6),

$$\frac{\mu_c}{\mu_b} = \frac{m_c/m_b}{S_c/S_b} \quad (7)$$

This means that if the cap-to-band sample ratio is normalised by the cap-to-band surface area ratio, it will be equal to the cap-to-band coating thickness ratio. Eq. (4) shows that when the cap-to-band projected area ratio is larger than the cap-to-band surface area ratio, the coating thickness on the cap is larger than that on the band, and vice versa. Therefore, when the cap-to-band sampling ratio (m_c/m_b) is larger than the cap-to-band surface area ratio (S_c/S_b), the coating thickness of the cap (μ_c) is larger than that on the band (μ_b), and *vice versa*.

2.2 Relative standard deviation (RSD) of coating thickness

The intra-tablet variability is generally defined as the relative standard deviation of the coating thickness distribution within a tablet (Freireich and Wassgren, 2010; Freireich *et al.*, 2015). In particular, if the coating thickness is distributed on different areas (*e.g.* triangular mesh elements or the cap and band) on a tablet, the average coating thickness can be defined as:

$$\bar{\mu} = \frac{1}{S} \sum_{i=1}^{N_f} \mu_i S_i \quad (8)$$

where S is the total surface area of the tablet; N_f is the total number of areas (triangles, see Table 1)

on the tablet; μ_i and S_i are the thickness and surface on area i . The relative standard deviation weighted by these areas (Freireich *et al.*, 2015) can be defined as:

$$\sigma = \frac{1}{\bar{\mu}} \sqrt{\frac{\sum_{i=1}^{N_f} S_i (\mu_i - \bar{\mu})^2}{S}} \quad (9)$$

Based on the cap-to-band ratios, a cap-to-band relative standard deviation (RSD) of an average tablet can be analysed. Assuming a uniform inter-tablet distribution and a uniform distribution on the cap and band respectively, according to Eqs. (2) and (3), the cap-to-band coating volume ratio is:

$$\frac{V_c}{V_b} = \frac{S'_c}{S'_b} = \alpha \quad (10)$$

$$\frac{S_c}{S_b} = \beta \quad (11)$$

If a uniform distribution on the cap and band is assumed, the cap-to-band relative standard deviation (weighed by the cap and band surface areas) can be defined as:

$$\begin{aligned} \sigma &= \frac{1}{\bar{\mu}} \sqrt{\frac{S_c (\mu_c - \bar{\mu})^2 + S_b (\mu_b - \bar{\mu})^2}{S_c + S_b}} \\ &= \frac{\beta + 1}{\alpha + 1} \sqrt{\frac{\beta \left(\frac{\alpha}{\beta} - \frac{\alpha + 1}{\beta + 1} \right)^2 + \left(1 - \frac{\alpha + 1}{\beta + 1} \right)^2}{\beta + 1}} \end{aligned} \quad (12)$$

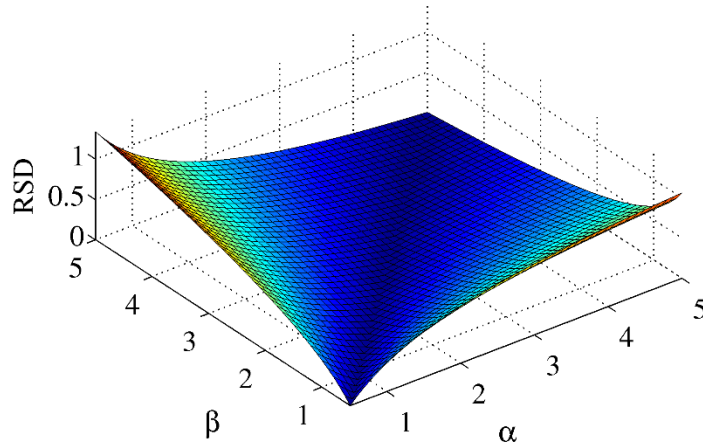


Figure 1: The cap-to-band relative standard deviation (RSD) with projected area ratio (α) and surface area ratio (β). The cap-to-band RSD is plotted as a function of α and β . The RSD is zero when α is equal to β , and increases with the difference between α and β .

Figure 1 shows the surface of cap-to-band relative standard deviation (RSD) as a function of α and β . The diagonal line in the α - β plane represents the fact that the RSD is equal to zero when α is equal to β . A larger difference between the surface area ratio and the projected area ratio can produce a relatively larger RSD. The cap-to-band RSD is equal to the intra-tablet variability when the coating thickness distributions are uniform on the cap and the band, respectively.

3. Simulation Methodology

3.1 DEM model of tablets in coating pan

In order to verify the relationship between the cap-to-band coating thickness ratio and the orientation properties of tablets in the rotating pan derived above, discrete element method (DEM) simulations were used to compute the dynamics of tablets in the coating pan. The spray process is not coupled directly to the tablet motion in DEM model, but based on the post-processing of tablet trajectories exported from DEM simulations.

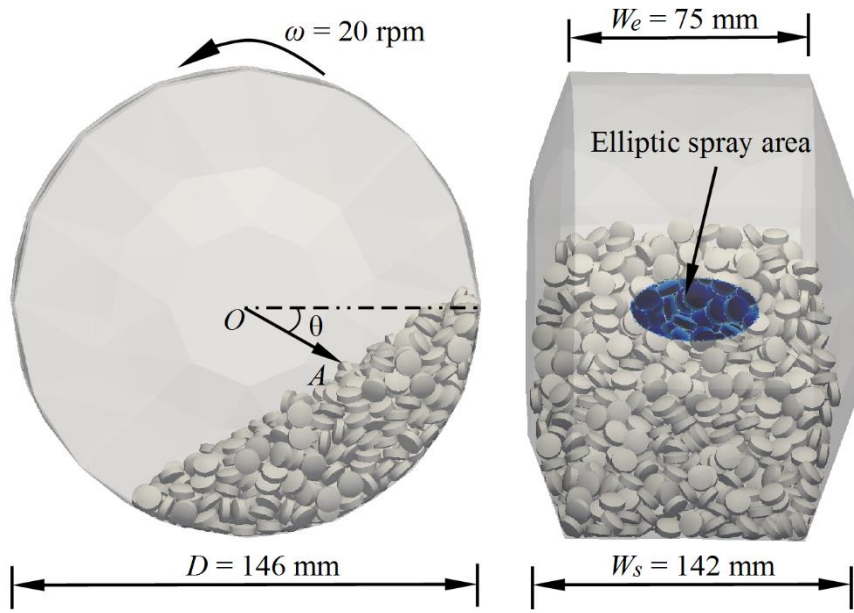


Figure 2: DEM model of the tablet bed in rotating pan. The vector OA indicates the spray direction with respect to the horizontal direction. Following the spray direction (OA), an elliptic spray area (highlighted in blue) is projected onto the tablet bed.

Table 1: Tablet shapes studied in DEM tablet coating simulations. Both the mesh representation (for spray coating) and multi-sphere representations (for DEM simulations) are shown.

Biconvex	Flat	Elliptic	Star

The DEM model of tablets in a rotating pan is illustrated in Figure 2. Four types of tablets were simulated, with different shapes: biconvex, flat cylinder, ellipse and rounded star polygon, as represented by surface meshes as shown in Table 1. All types of tablets were defined to have identical volume and density in order to generate the same fill ratio in the pan. The actual size of the tablets varied with their shape, with maximum diameters in the range of 4 to 8 mm and thicknesses

in the range of 3 to 4 mm. The material properties of the tablet and the pan, as shown in Table 2, are typical of values for polymeric tablet cores and stainless steel pan. In the DEM model, the shape of the tablets was represented using a multi-sphere method. Depending on the shape of the tablet, the multi-sphere is constructed from 6 to 14 rigidly connected primary spheres (Pei *et al.*, 2015), as shown in Table 1. The difference between the meshed tablet (in semi-transparent colour) and the multi-sphere tablet representations is also illustrated in Table 1. The multi-spheres are used in DEM simulation for the dynamics of tablets, while the meshed tablets are used for the spray coating in the image analysis method. Theoretical studies (Höhner *et al.*, 2011) indicate that the temporal force evolution of the multi-sphere model shows some differences from that of the meshed model (polyhedron) during collisions. However, the polyhedron model is extremely expensive for computation. In addition, recent researches (Pasha *et al.*, 2016) have shown that the multi-sphere model can achieve statistical agreement with the experiments in particle mixing/blending. Therefore, the multi-sphere model was chosen for DEM simulations in this study.

The tablets were initially generated at random positions and orientations and deposited under gravity into the pan, which was rotated at a speed of 20 rpm. The Froude number of the mixing process in the pan, which is defined as the centrifugal acceleration divided by the gravitational acceleration, is 0.016, which indicates the flow pattern of the mixing process is in the rolling/cascading regime (Mellmann, 2001). The total simulation time was approximately 60 seconds, and the simulation time step was 10^{-6} s. The position and quaternion orientation of the multi-sphere particles (tablets) in DEM model were exported every 0.05 seconds to obtain the corresponding surface mesh representation for determination of coating thickness.

Table 2: Material properties and process conditions (Hancock *et al.*, 2010; Suzzi *et al.*, 2012)

Parameter	Value
Number of tablets	1000
Tablet density	1300 kg m ⁻³
Tablet mass	~ 200 mg
Tablet Young's modulus	5.0 GPa
Pan bulk density	7800 kg m ⁻³
Pan Young's modulus	210 GPa
Tablet and pan Poisson ratios	0.3
Coefficient of friction (tablet-tablet)	0.74
Coefficient of friction (tablet-pan)	0.74
Coefficient of restitution	0.74
Spray angle (θ)	30°, 60°
Number of pixels in spray area	~ 250000
Spray volume rate per pixel (ζ)*	10 ⁻¹³ (m ³ s ⁻¹)

* Wet spray rate: $\zeta = 7.5 \text{ g min}^{-1}$, considering the density of coating material is 1000 kg m⁻³ in 20% w/w water soluti

The DEM simulation is implemented in LIGGGHTS 3.1.0 (Kloss *et al.*, 2012) with classical contact mechanics – Hertz theory for the normal contacts (Johnson, 1985) and Mindlin theory for the tangential contacts (Mindlin, 1949). The interaction parameters, especially the coefficient of friction, vary with the material type, as reported by previous experimental studies (Hancock *et al.*, 2010; Suzzi *et al.*, 2012). Hancock *et al.* (2010) suggested that the tablet-polymer/steel friction coefficient varies from 0.0 to 0.74 according to the material and surface properties. Suzzi *et al.* (2012) showed that the coefficient of restitution between tablets and a marble plate is 0.74±0.03. In the current study, since the coating pan is not equipped with baffles, the coefficient of friction is set to the relatively higher value of 0.74, following Hancock *et al.* (2010). However, it should be noted that the influence of interaction parameters, especially the coefficient of friction, on the tablet orientation and intra-tablet coating thickness distribution requires further investigation in future.

3.2 Tablet spray coating method

The spray coating process, based on an image analysis method introduced by Freireich *et al.* (2015), was applied to the tablet trajectories generated from DEM simulations. In this method, the tablets are shown in a 2D image rendered from a 3D scene. The image pixels in a specified spray zone area are treated as spray droplets. When a tablet appears in the specified spray zone in the image, the pixels that are rendering the corresponding areas of the tablet are considered to be coated onto these areas of the tablet. In order to track the appearance of tablets in the spray area, the tablet surface is meshed by triangular elements as shown in Table 1. The ID of the triangular element in the tablet system is defined as:

$$p_{ij} = iN_p + j \quad (13)$$

where N_p is the total number of triangular elements on the tablet; i is the ID of the tablet; j is the index number of the triangular element on the tablet, ranging from 0 to $N_p - 1$. The position and quaternion orientation of tablet are mapped from the multi-sphere representation to the meshed representation. In other words, for the output frames, the position and orientation of meshed tablets and multi-sphere tablets will be identical. Then, each triangular element is mapped to a unique colour as shown in Figure 3 so that it is possible to identify whether or not the triangular element is rendered in the spray zone by this unique colour (pixel). The RGB (Red-Green-Blue) colour of each triangular element is calculated as:

$$R = p_{ij} \% 255 \quad (14)$$

$$G = \begin{cases} \left[\frac{p_{ij}}{255} \right] & p_{ij} < 65025 \\ \left[\frac{p_{ij}}{255} \right] \% 255 & p_{ij} \geq 65025 \end{cases} \quad (15)$$

$$B = \left[\frac{p_{ij}}{65025} \right] \quad (16)$$

where % is the modulus operator which finds the remainder after the division, and [] is the truncation operator which finds the integer part of argument after the division. Using this method, each colour component varies from 0 to 254. In OpenGL, when the colour component is larger than 255, it will be truncated to 255. Therefore, to ensure that the colour is unique for each triangular element, the green (G) colour must be assigned according to the ID of the triangular element as illustrated in Eq. (15). The colour white ($\{R \ G \ B\} = \{255 \ 255 \ 255\}$) is reserved for the background. Using this index method, the number of triangular elements can be up to 255^3 , which is sufficient for the number, size and shape of tablets in the simulations. Accordingly, the ID of the triangular element can be retrieved from the RGB colour as:

$$p_{ij} = 65025B + 255G + R \quad (17)$$

Therefore, the surfaces of tablets in the spray area can be uniquely identified according to the colour of the pixel in the spray area. It should be mentioned that the OpenGL will run a depth test to show only the surface elements in front of others when there is an overlay of surfaces. In other words, only surfaces that have direct intersections with spray rays will be coated, whereas others behind the coated surface will not. In this study, an elliptic spray area (40 mm by 20 mm in diameter) as shown in Figure 3 is applied on to the tablet bed, with a spray direction OA making an angle θ with respect to the horizontal direction, as shown in Figure 2.

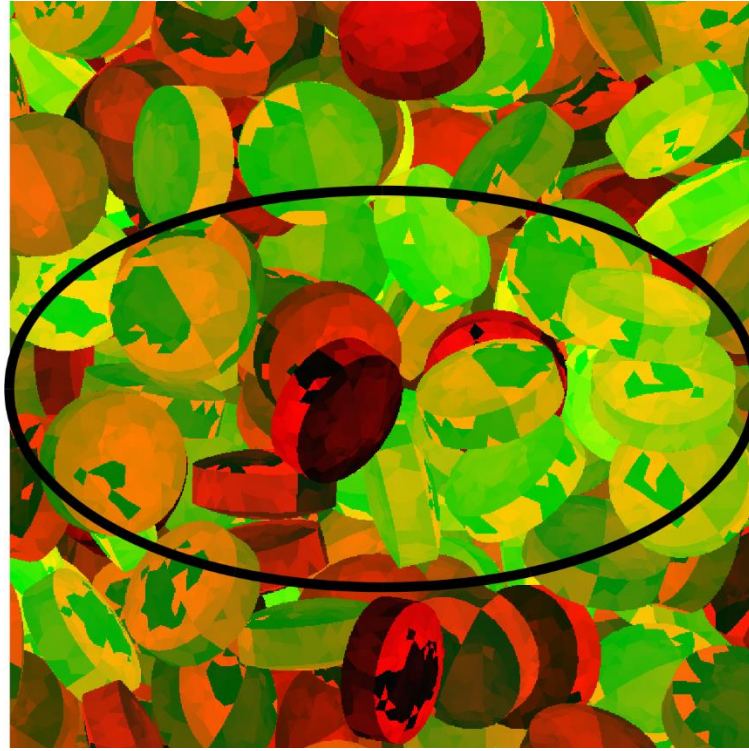


Figure 3: 2D projection of tablets and spray zone area (black ellipse) on surface of bed, as seen parallel to the spray direction. Triangular mesh elements are indexed by different colours. The Figure size is 800×800 (pixels). So, the total number of pixels is 640,000 and the number of pixels in the elliptic spray area ($40 \text{ mm} \times 20 \text{ mm}$) is about 250,000.

For each frame exported from DEM simulation, corresponding to a 0.05 second time increment, the triangular elements in the spray zone area are coated, and the incremental coating thickness on the corresponding triangular element is calculated as:

$$h_{ij}^t = \frac{n_{ij}^t V_p \Delta t}{A_{ij}} \quad (18)$$

where h_{ij}^t is the incremental coating thickness on the triangular element p_{ij} at time instant t ; n_{ij}^t is the number of spray rays (pixels) in the triangular element; V_p is the spray volume rate of the coating material (solute) per each pixel; Δt is the output time interval and A_{ij} is the area of the triangular element. The coating thickness of the triangular element, h_{ij} , is the accumulation of the

incremental coating thickness over all time instants.

In the current study, the average tablet (Freireich *et al.*, 2015) is used to represent the intra-tablet coating thickness distribution and calculate the cap-to-band coating thickness ratio. The mean coating thickness of each triangular element on the average tablet is defined as:

$$h_j = \frac{\sum_{i=1}^N h_{ij}}{N} \quad (19)$$

where N is the number of tablets. The mean coating thickness of each triangular element on the average tablet is the average value of the coating thickness of triangular elements with the same index number j on all tablets. Then the mean coating thickness on the cap and band of the average tablet can be computed as:

$$\mu_c = \frac{\sum_j^{N_c} h_j^c A_j^c}{\sum_j^{N_c} A_j^c} \quad (20)$$

$$\mu_b = \frac{\sum_j^{N_b} h_j^b A_j^b}{\sum_j^{N_b} A_j^b} \quad (21)$$

where h_j^c and A_j^c are the coating thickness and area of the triangular element on the cap while h_j^b and A_j^b are on the band. Therefore, the cap-to-band coating thickness ratio is μ_c / μ_b .

3.3 Ray-tracing sampling method for cap-to-band ratio

The ray-tracing sampling method (Toschkoff *et al.*, 2013; Toschkoff *et al.*, 2015) is also applied to analyse output frames at various time instants to obtain the cap-to-band sample ratio. Two types of rays are constructed, as shown in Figure 4. In the first type, the direction of the ray follows the elliptic cylinder. According to the image analysis method shown in Figures 2 and 3, the pixels in the elliptic spray area are considered as the intersection point between the droplet and tablet. If the elliptic spray area is extruded following the spray direction, an elliptic cylinder will be formed as shown in Figure 4. Therefore, the ray in (following) the elliptic cylinder to obtain sampling points on tablets is used to mimic the image analysis method. In the other type, the direction of the ray follows the actual spray direction, which is from the nozzle at the centre of the drum to the elliptic spray area. This forms an elliptic cone and the rays in (following) the elliptic cone is used to mimic the actual spray zone.

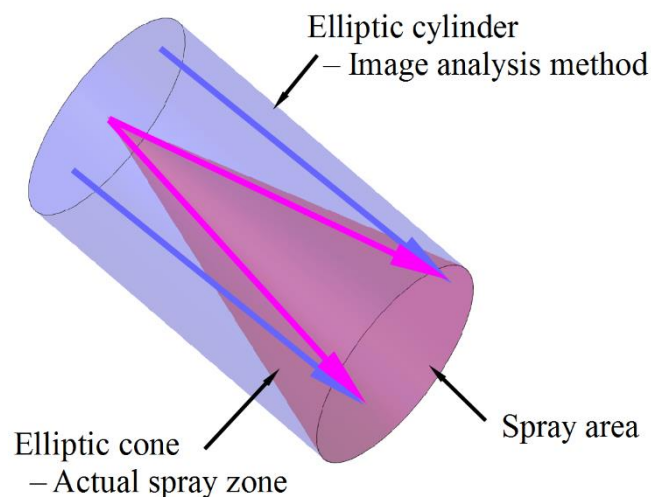


Figure 4: The construction of the two types of rays for determining cap-to-band ratio. The first ray type (blue) follows the elliptic cylinder to mimic the image analysis method; the second ray type (magenta) follows the elliptic cone to mimic the actual spray zone.

The cap-to-band sample ratio varies with the number of rays, as shown in Appendix A. This is due to the random movement of tablets in the drum. However, when the number of rays (sampling points) of each type is large enough, the cap-to-band (normalized) sample ratio becomes stable and is in excellent agreement with the cap-to-band coating thickness ratio (relative error < 3%), as shown in Appendix A. In this study, for each output frame, six randomly generated rays of each type

are projected into the elliptic spray area on the tablet bed following their corresponding directions. For each ray, the first triangular element that has an intersection point with that ray is recorded, and the corresponding element then analysed to determine whether it is on the cap or band of the corresponding tablet. From output frames at various time instants, the cap-to-band sample ratio, which is the ratio of the number of intersections on the cap to that on the band, can be calculated from more than 6,000 intersection points. This ray-tracing sampling method is used to further analyse the intra-tablet coating thickness distribution by comparing the cap-to-band coating thickness ratio and sample ratio.

Both the image analysis method and the ray-tracing method are based on the output of DEM simulations. In the image analysis method, the spray area on the tablet bed is fully covered by the pixels which represents the spray droplets. The spray zone demonstrated by the image analysis method is an elliptic cylinder as shown in Figure 4. In the ray-tracing method, the ray represents the trajectory of the droplet. An arbitrary number of rays and angles can be used to sample the tablet bed. Therefore, the ray-tracing method can be more flexible and able to follow the actual spray zone which is an elliptic cone in this study. The image analysis method is more computationally efficient than the ray-tracing method, especially when a large number of rays are involved, since the depth test in image analysis is done during the rendering of the 2D image. However, none of the methods used in this study can consider the effects of using real liquid droplets to coats the tablets, such as the spreading and drying of liquid on the tablets (Ruotsalainen *et al.*, 2003, Suzzi *et al.*, 2010) and capillary forces (Nase *et al.*, 2001) during the coating and mixing process. The liquid bridges and capillary forces between wet tablets can alter the flow pattern during the spray coating process, and consequently these phenomena will influence the orientation distribution of tablets. Therefore, the cap-to-band coating thickness ratio may vary and defects and liquid transfer between wet coating surfaces can also occur. The research of these phenomena are beyond the scope of current numerical models and need further investigation.

4. Results and discussion

4.1 The spray coating process

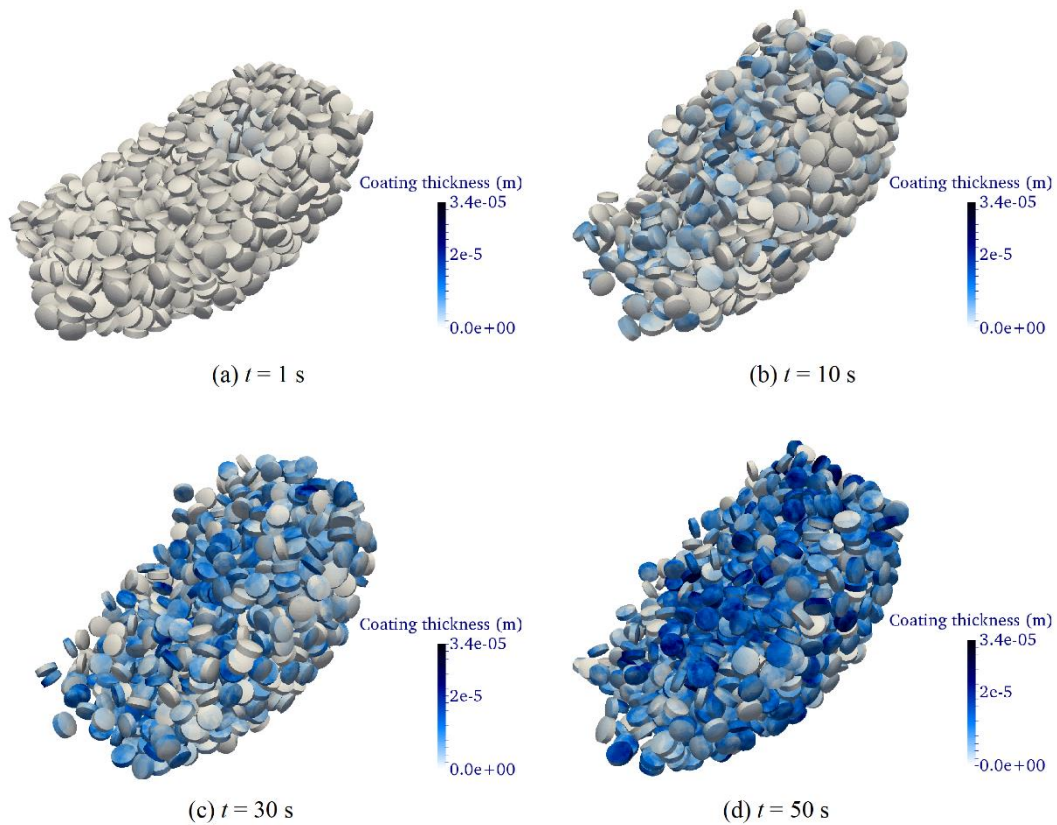


Figure 5: The progress of spray coating process at various time instants during simulation. The coating material is sprayed onto the tablet bed while tablets move and mix in the rotating drum. The darkness of the blue colour on tablets shows the coating thickness on each triangular panel. The average coating thickness generally increases with the coating time, from (a) to (d).

Figure 5 shows the results of spray coating process of biconvex tablets modelled by DEM and image analysis method described above. During the process, tablets in the spray zone area accumulate coating on their surface, as can be seen from Figure 5a. With the rotation of the drum, tablets cascade down the tablet bed and migrate inside the coating pan. Thus, other tablets can enter

the spray zone, accumulate the coating material on their surfaces and leave the spray zone according to their movement through the drum. Consequently, while the total coating thickness (volume) increases steadily with time, tablets with different coating thickness are distributed in the pan, as shown in Figures 5b, 5c and 5d. More importantly, the coating thickness also varies on the surface of each individual tablet. In other words, both intra- and inter-tablet coating thickness distributions are observed from the simulations.

4.2 Cap-to-band ratios

Figure 6 presents the intra-tablet coating thickness distribution of the average tablets (*i.e.* taken as arithmetic mean of each triangular element over all tablets in simulation) at different spray angles (30° and 60°) after 60 s. Generally, the coating thickness is relatively larger on the band at a small spray angle of 30°, while the cap has the larger coating thickness at a large spray angle of 60°. The evolution of cap-to-band coating thickness ratio of the average biconvex tablet is given in Figure 7. It can be seen that after a few seconds of coating, the cap-to-band coating thickness ratio converges to an asymptotic value. For the small spray angle of 30°, the asymptotic value is lower than one, which indicates the mean coating thickness on the cap is smaller than that on the band. On the other hand, the large spray angle of 60° causes the ratio larger than one and a larger coating thickness on the cap. The convergence of the cap-to-band coating thickness ratio is in good agreement with the analysis of the intra-tablet variability by Freireich *et al.* (2015), in which the intra-tablet variability of the average tablet rapidly approaches an asymptotic limit within 100 coating trials.

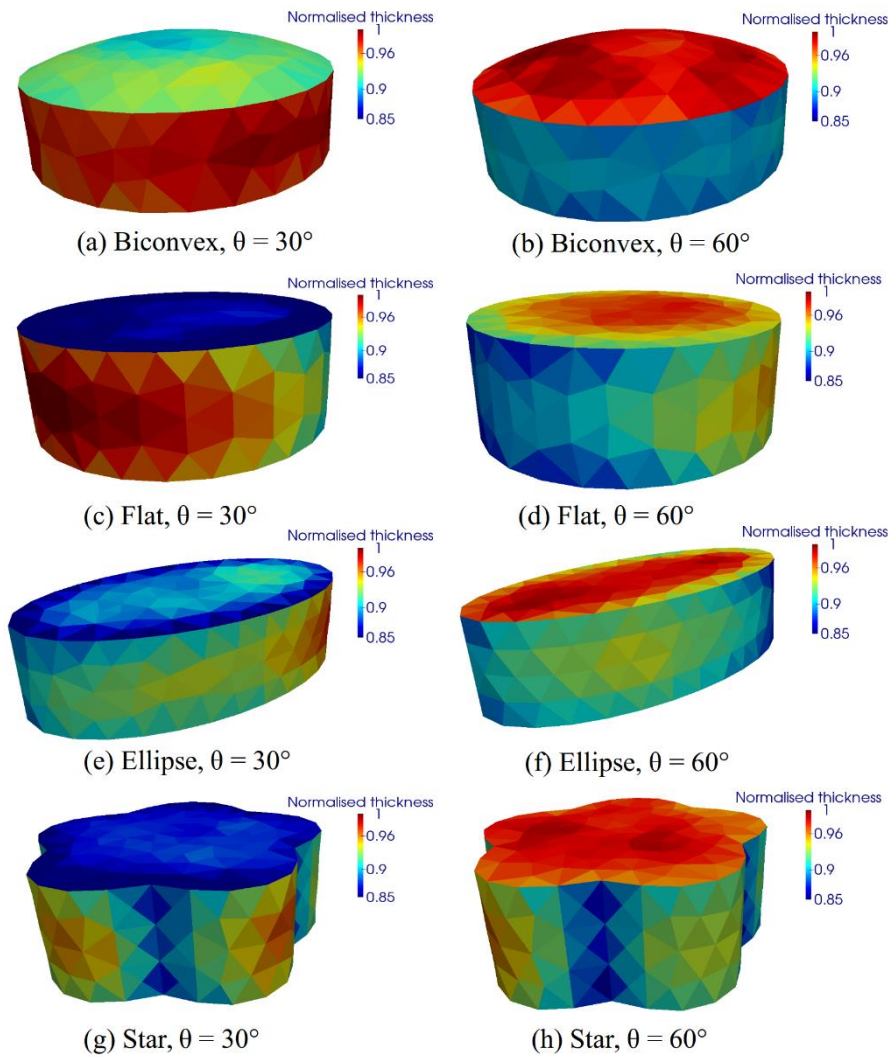


Figure 6: The coating thickness distributions on average tablets of various shapes and spray angles. The coating thickness is normalised by the maximum coating thickness of each average tablet. For all shapes, the coating thickness on the band is larger when $\theta = 30^\circ$ but smaller when $\theta = 60^\circ$.

Figure 8 shows the evolution of the cap-to-band sample ratio of biconvex tablets obtained from the ray-tracing sampling method. The dash line gives the cap-to-band surface area ratio. The cap-to-band sample ratio initially fluctuates and gradually becomes relatively stable as the number of samples increases. The cap-to-band sample ratio at the small spray angle of 30° is lower than the surface area ratio while the one at large spray angle of 60° is higher. This indicates that with the large spray angle, more rays hit the cap than the band on tablets, which shows the same tendency as the cap-to-band coating thickness accumulation modelled by the image analysis method. The cap-to-band coating thickness and sample ratios of other types of tablets have a similar trend as for the biconvex tablets.

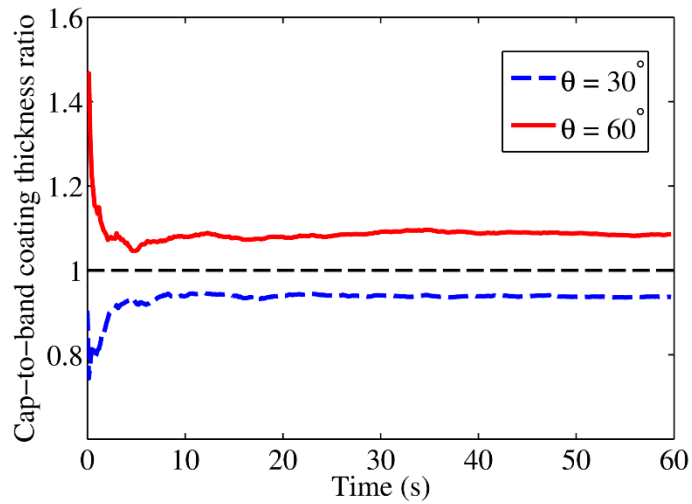


Figure 7: The time evolution of the cap-to-band coating thickness ratio of the average biconvex tablet. This thickness ratio converged rapidly with time during the spray coating process. It is smaller than one ($\mu_c < \mu_b$) when spray angle, $\theta = 30^\circ$ (blue dash line) but larger than one ($\mu_c > \mu_b$) when $\theta = 60^\circ$ (red solid line). Tablets with shapes other than biconvex also showed similar trends.

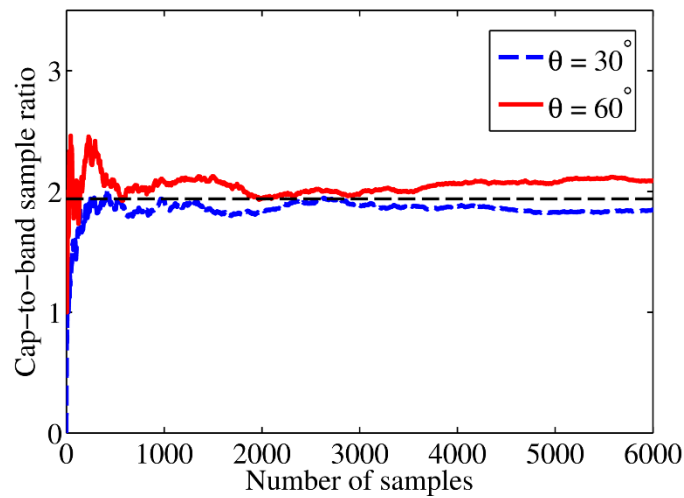


Figure 8: The time evolution of cap-to-band sample ratio of biconvex tablets in the ray-tracing sampling process. This sample ratio becomes stable with the increase of the number of samples. It is smaller than one ($m_c < m_b$) when $\theta = 30^\circ$ (blue dash line) but larger than one ($m_c > m_b$) when $\theta = 60^\circ$ (red solid line). Tablets with shapes other than biconvex also showed similar trends.

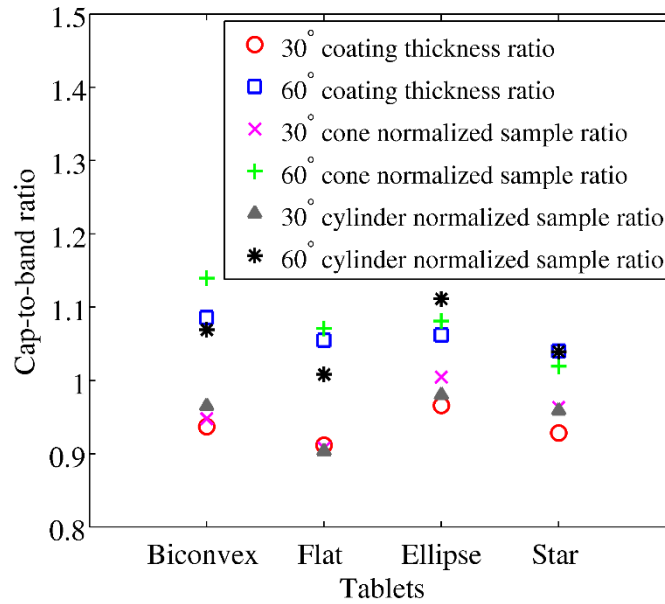


Figure 9: The cap-to-band coating thickness ratios and normalised sample ratios for tablets of different shape (Table 1). The cap-to-band sample ratios are generated from both rays following the elliptic cone and elliptic cylinder. The cap-to-band normalised sample ratio agrees with the corresponding cap-to-band coating thickness ratio for all shapes. The spray angle of 30° causes the ratios larger than one, while 60° makes the ratios smaller than one.

Figure 9 shows the cap-to-band coating thickness ratio and normalised sample ratio. The cap-to-band coating thickness ratio is calculated from the image analysis method (see Section 3.3), in which each pixel in the spray zone represents a unit area of the project area of a tablet and a droplet with a unit volume at the same time. Therefore, the cap-to-band coating thickness is equal to the cap-to-band projected area normalised by the cap-to-band surface area as illustrated by Eq. (4). According to Eq. (7), the normalised cap-to-band sample ratio should be equal to the cap-to-band coating thickness ratio (i.e. normalised cap-to-band projected area ratio). In Figure 9, it can be seen that the normalised cap-to-band sample ratio can generally agree with the cap-to-band coating thickness ratio with small relative errors ($< 5\%$), as the normalised cap-to-band sample ratios are calculated from 6 randomly generated rays. Nevertheless, it is found that, in order to obtain a cap-to-band coating thickness ratio of unity, the cap-to-band projected area ratio should be equal to the cap-to-band surface area ratio. In Pérez-Ramos's experimental study (2007) discussed in Section 1,

the orientation index which is the ratio of the band-to-cap exposed (projected) area ratio to the surface area ratio varies with the pan speed, air flow, and fill ratio. The orientation index is generally smaller than one, which indicates the cap is more exposed than the band to the high speed camera. The orientation index can increase as the pan speed and fill ratio increase. The inlet air flow can affect the tablet orientation and decrease the orientation index when the pan speed is relatively small (*e.g.* less than 12 rpm).

Similar experimental results were obtained by Kandela *et al.* (2010) using tracer tablets, in which the cap and band were painted with different colours, instead of all tablets for the video imaging analysis. It was found that the calculated band-to-cap weight gain ratio using a Monte Carlo algorithm generally increased as the normalised band-to-cap projected area ratio increased. However, the effect of the angle of the high speed camera (spray direction) was unclear in the experimental study. From Figure 9, it can be seen that a spray angle of 30° results in cap-to-band ratios larger than one, indicating the cap has a larger coating thickness, while 60° results in the ratios becoming smaller than one. Nevertheless, both the experimental and numerical studies agree that the tablets in the spray coating process has a preferred orientation which can be characterized by the cap-to-band projected area ratio divided by the cap-to-band surface area ratio.

This theoretical rule is generally applicable to both convex and concave tablets. However, only the mean values of coating thickness on the cap and band are used as shown in Eq. 4, and so intra-coating thickness distributions on the cap and band can still be observed. For instance, on the band of the star tablet as shown in Figure 6, the convex corners (tips) have a larger coating thickness than the concave area. This is because the convex corners tend to block the spray in way to the concave surface and accumulate more coating materials.

In this study, an optimum spray angle should produce the cap-to-band coating thickness ratio of 1.

From Figure 9, it can be seen the cap-to-band ratio varies with the particle shape. For instance, the elliptic tablet at the spray angle of 30° can have the cap-to-band coating thickness ratio close to 1, while the cap-to-band coating thickness ratio of the flat cylindrical tablet at the same spray angle is much smaller. Therefore, for the flat cylindrical tablet using a linear approximation, the optimum angle should be in the range of $40^\circ - 50^\circ$. In addition, it is worth mentioning that the process conditions, such as the friction, rotation speed and fill ratio can also influence the cap-to-band coating thickness ratio. Since this study mainly focuses on the relationship of the cap-to-band coating thickness ratio, projected area ratio and sampling ratio, the combined effects of spray angle and other process conditions will be investigated in order to predict the optimum spray angle in further studies.

4.3 Asymptotic limits

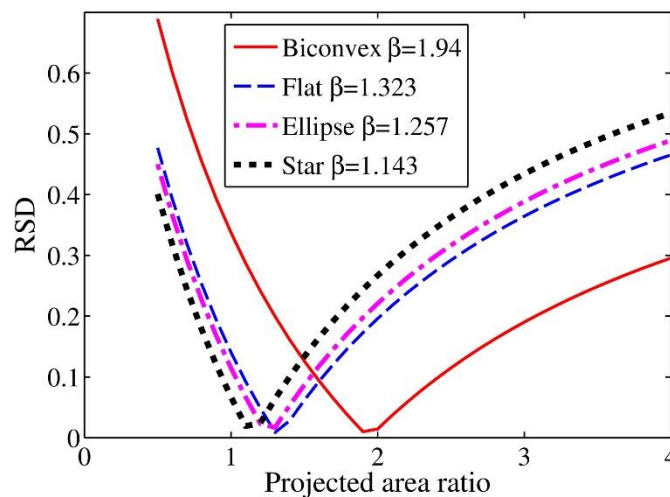


Figure 10: The cap-to-band RSD of tablets. The RSD is plotted as a function of cap-to-band projected area ratio, α , which is a slice through the 2D surface shown in Figure 1. The values of β for the various tablets of different shape are also listed. The RSD is zero when α is equal to β and increases with the difference between α and β .

Figure 10 shows the RSD of various tablets as a function of projected area ratio, α , according to Eq. (12). The RSD is zero when α is equal to the actual area ratio, β , and increases with the difference

between α and β . For example, considering the biconvex tablet, for α in the range from 1.7 to 2.2 (see Figure 10), the RSD varies from 0.064 to 0.0 (with α from 1.7 to 1.94) and from 0.0 to 0.058 (with α from 1.94 to 2.2). The analysis of this simple RSD indicates that during the coating process, the asymptotic value of intra-tablet distribution will be achieved when the inter-tablet coating thickness distribution and the coating distribution on the cap and band becomes uniform. On the other hand, it should be noted that even when this simple RSD achieves a zero value, it does not necessarily mean that the intra-tablet coating thickness distribution is zero. As discussed above, uniform distributions on the cap and band are assumed in this analysis. However, for instance, especially for concave (star) tablets as shown in Figure 6, the coating thickness distribution on the band can be non-uniform, although the mean coating thickness on the band can be equal to that on the cap, depending on the projected area ratio and surface area ratio.

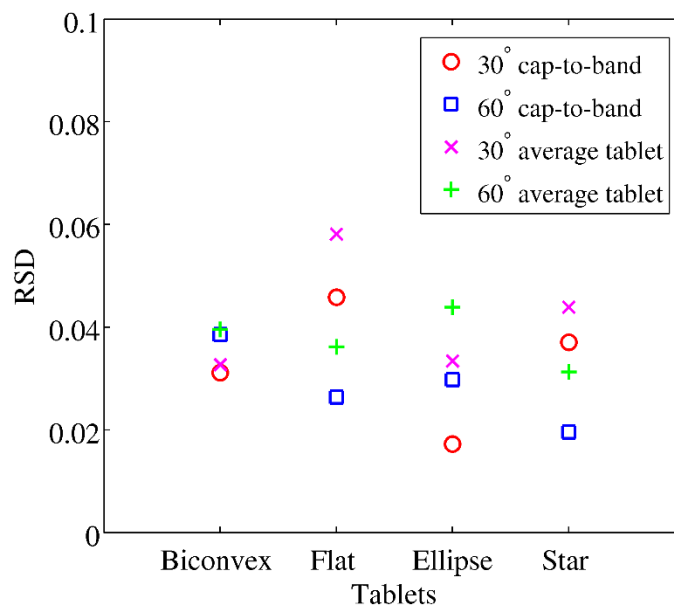


Figure 11: The RSDs calculated from cap-to-band ratios and average tablets. The cap-to-band projected area ratio is obtained by multiplying the cap-to-band thickness ratio by the cap-to-band surface area ratio (Biconvex: 1.94; Flat: 1.323; Ellipse: 1.257; Star: 1.143), according to Eq. 4. The differences between the RSDs calculated from cap-to-band ratios (Eq. 14) and from average tables (Eq. 11) are within 2%.

Figure 11 presents the comparison between the RSDs calculated from cap-to-band ratios and average tablets. In general, the RSDs calculated from average tablets according to Eq. (9) are slightly larger than those calculated from cap-to-band ratios according to Eq. (12). For Eq. (12), the coating thickness distributions are assumed to be uniform on both cap and band. However, in the average tablet in Figure 6, the coating thickness is not entirely uniform on the cap and band. Therefore, the intra-tablet variability of the average tablet is slightly larger than the cap-to-band RSD. Nevertheless, the differences are within 2%, which indicates that cap-to-band ratio RSD is capable to predict the asymptotic limit of the intra-tablet variability, especially when the coating thickness distributions are relatively uniform on the cap and band. It is interesting to notice that the RSD varies with the spray angle, depending on the shape of the tablet. For instance, a spray angle of 30° causes a slightly larger RSD for the biconvex shaped tablet but a smaller RSD in the flat cylinder and star-shaped tablets, compared with their corresponding spray angle of 60°. In this paper, the cap-to-band coating thickness ratio is directly related to the orientation of tablets (e.g. cap-to-band projected area ratio) regardless the flow pattern. However, the particle shape can influence the motion and orientation of particles during the mixing, which will also lead to various cap-to-band projected area ratio, although the general flow pattern of the mixing process for various particle shapes is in rolling/cascading regime (Mellmann, 2001). The effects of particle shape and process conditions on the flow pattern and orientation of tablets will be investigated in future work.

4.4 The effect of spray angle on coating thickness distributions

In the current study, a smaller spray angle of 30° causes a larger coating thickness on the band while a larger spray angle of 60° produces a larger coating thickness on the cap. These results are in broad agreement with investigations by Ketterhagen (2011) and Freireich *et al.* (2011). Ketterhagen (2011) showed that a geodesic mean can be calculated based on the distribution of the major axes of tablets, which indicates that statistically tablets on the free surface of the tablet bed have an

orientational preference in the rotating drum, as illustrated in Figure 12. When the spray angle is smaller, the projected area of the band can become larger and the RSD or intra-tablet variability can decrease as the cap-to-band projected area ratio is still larger than the cap-to-band surface area ratio according to Figure 12. This explains the observation by Ketterhagen (2011) and Freireich *et al.* (2011) whereby the intra-tablet variability is decreased by changing the spray angle, but the coating thickness on the cap is still generally larger than that on the band. However, in the current study, when the projected area of the band is large enough at the spray angle of 30°, the cap-to-band RSD or the intra-tablet variability starts to increase (Figures 10 and 11) and the coating thickness on the cap is smaller than that on the band as the cap-to-band projected area ratio becomes smaller than the cap-to-band surface area ratio. This could be caused by the larger coefficient of friction used in the simulation, as a larger friction can introduce a higher tablet bed and a larger angle of repose during the rotation. The orientations of the tablets are thereby influenced and consequently the band of the tablet exposes larger area to the spray direction at the small spray angle used in the current study.

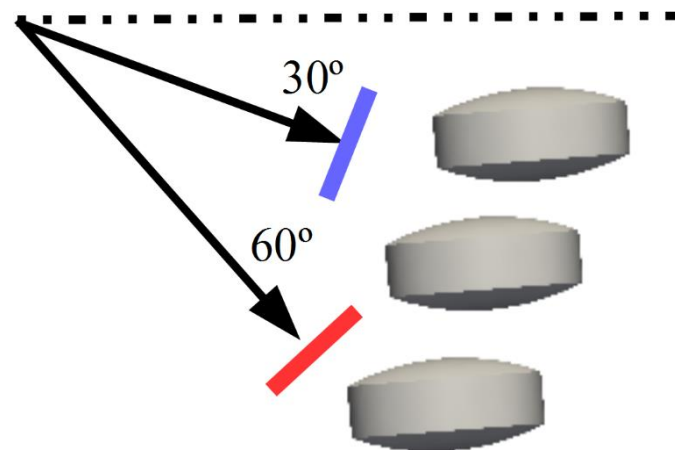


Figure 12: The illustration of the spray and the orientation preference of tablets. The blue and red segments indicate the spray areas (planes) for different spray directions. The tablets with preferred orientations expose different projected area to different spray directions.

5. Conclusions

In this study, the effect of the orientation of tablets on the cap-to-band coating thickness distribution in a rotating pan was investigated. The dynamics of tablets in the pan was modelled using DEM, while the image analysis method based on the output of DEM was applied to model the spray coating process and analyse the cap-to-band coating thickness ratio. The ray-tracing sampling method was further used to obtain the cap-to-band sample ratio. The cap-to-band RSD was subsequently estimated based on the cap-to-band projected area ratio and surface area ratio. A theoretical analysis shows that the cap-to-band coating thickness ratio should be equal to the quotient of the cap-to-band projected area ratio and the cap-to-band surface area ratio. It was confirmed by DEM simulations that the cap-to-band coating thickness ratio is indeed equal to the cap-to-band projected area ratio divided by the cap-to-band surface area ratio, in agreement with the theoretical analysis. When the cap-to-band projected area ratio is larger (or smaller) than the cap-to-band surface area ratio, the mean coating thickness on the cap is larger (or smaller) than that on the band. The theoretical analysis also indicates that the cap-to-band coating thickness ratio should be equal to the normalised cap-to-band sample ratio obtained from the ray tracing sampling method. The spray angle plays an important role in controlling the spray coating process. A small spray angle with respect to the horizontal direction can decrease, and even invert the cap-to-band coating thickness ratio, leading to a larger coating thickness on the band than on the cap. Nevertheless, an asymptotic value of cap-to-band RSD is still reached once the cap-to-band coating thickness ratio becomes stable during the coating process. These findings can be generally applicable in helping to reduce coating variability of pharmaceutical tablets of various shapes. Further theoretical analysis and experimental studies on the effects of friction should be considered in future.

Acknowledgements

The authors would like to acknowledge financial support from UK EPSRC Research Grant

EP/L019787/1 and EP/L019922/1. Additional data related to this publication is available at the University of Cambridge data repository (<https://doi.org/10.17863/CAM.10704>).

Appendix A : Correspondence of the cap-to-band sample and coating thickness ratios

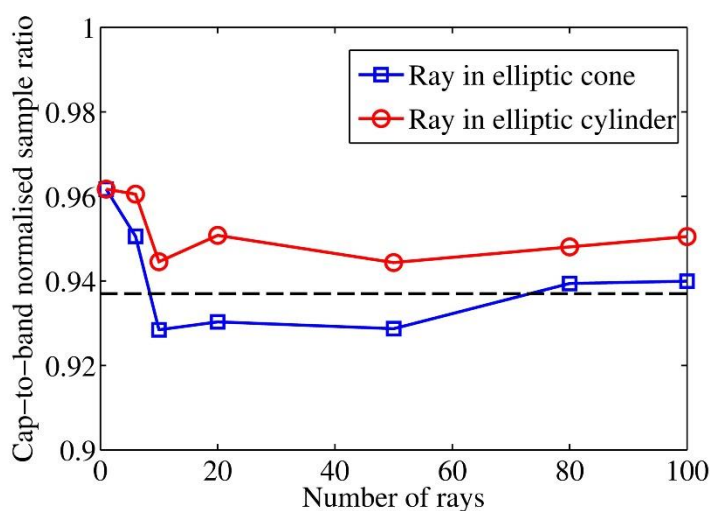


Figure A1: The normalised cap-to-band sample ratios for biconvex tablets as a function of the numbers of rays. The dashed line is the cap-to-band coating thickness ratio. In general, the cap-to-band normalised sample ratio agrees well with the cap-to-band coating thickness ratio, irrespective of the number of rays.

Figure A1 shows the influence of the number of rays on the cap-to-band normalised sample ratio using the ray-tracing method. The normalised cap-to-band sample ratio varies with the number of rays for both types (elliptic cone and cylinder). The difference between the cap-to-band normalised sample ratio and coating thickness ratio decreases slightly as the number of rays increases.

However, in general, the cap-to-band normalised sample ratio agrees well with the cap-to-band coating thickness ratio (relative error < 3%), even with a small number of rays.

References

- Brock, D., Zeitler, J.A., Funke, A., Knop, K., Kleinebudde, P., 2013a. Evaluation of critical process parameters for inter-tablet coating uniformity of active-coated GITS using Terahertz Pulsed Imaging. *Eur. J. Pharm. Biopharm.* 85, 1122–1129. doi:10.1016/j.ejpb.2013.07.004
- Brock, D., Zeitler, J.A., Funke, A., Knop, K., Kleinebudde, P., 2013b. Evaluation of critical process parameters for intra-tablet coating uniformity using terahertz pulsed imaging. *Eur. J. Pharm. Biopharm.* 85, 1122–1129. doi:10.1016/j.ejpb.2013.07.004
- Freireich, B., Ketterhagen, W.R., Wassgren, C., 2011. Intra-tablet coating variability for several pharmaceutical tablet shapes. *Chem. Eng. Sci.* 66, 2535–2544. doi:10.1016/j.ces.2011.02.052
- Freireich, B., Kumar, R., Ketterhagen, W., Su, K., Wassgren, C., Zeitler, J.A., 2015. Comparisons of intra-tablet coating variability using DEM simulations, asymptotic limit models, and experiments. *Chem. Eng. Sci.* 131, 197–212. doi:10.1016/j.ces.2015.03.013
- Freireich, B., Wassgren, C., 2010. Intra-particle coating variability: Analysis and Monte-Carlo simulations. *Chem. Eng. Sci.* 65, 1117–1124. doi:10.1016/j.ces.2009.09.066
- Hancock, B.C., Mojica, N., John, -Green K St, Elliott, J. a., Bharadwaj, R., 2010. An investigation into the kinetic (sliding) friction of some tablets and capsules. *Int. J. Pharm.* 384, 39–45. doi:10.1016/j.ijpharm.2009.09.038
- Ho, L., Müller, R., Römer, M., Gordon, K.C., Heinämäki, J., Kleinebudde, P., Pepper, M., Rades, T., Shen, Y.C., Strachan, C.J., Taday, P.F., Zeitler, J. A., 2007. Analysis of sustained-release tablet film coats using terahertz pulsed imaging. *J. Control. Release* 119, 253–261. doi:10.1016/j.jconrel.2007.03.011
- Höhner, D., Wirtz, S., Kruggel-Emden, H., Scherer, V., 2011. Comparison of the multi-sphere and polyhedral approach to simulate non-spherical particles within the discrete element method:

Influence on temporal force evolution for multiple contacts. *Powder Technol.* 208, 643-656.

Johnson, K.L., 1985. *Contact Mechanics*. Cambridge University Press, Cambridge.

Kandela, B., Sheorey, U., Banerjee, A., Bellare, J., 2010. Study of tablet-coating parameters for a pan coater through video imaging and Monte Carlo simulation. *Powder Technol.* 204, 103–112.
doi:10.1016/j.powtec.2010.07.024

Ketterhagen, W.R., 2011. Modeling the motion and orientation of various pharmaceutical tablet shapes in a film coating pan using DEM. *Int. J. Pharm.* 409, 137–149.
doi:10.1016/j.ijpharm.2011.02.045

Kloss, C., Goniva, C., Hager, A., Amberger, S., Pirker, S., 2012. Models , algorithms and validation for opensource DEM and CFD-DEM. *Prog. Comput. Fluid Dyn.* 12, 140–152.
doi:10.1504/PCFD.2012.047457

Kodam, M., Bharadwaj, R., Curtis, J., Hancock, B., Wassgren, C., 2009. Force model considerations for glued-sphere discrete element method simulations. *Chem. Eng. Sci.* 64, 3466–3475.

Lin, H., Dong, Y., Shen, Y., Zeitler, J.A., 2015. Quantifying Pharmaceutical Film Coating with Optical Coherence Tomography and Terahertz Pulsed Imaging: An Evaluation. *J. Pharm. Sci.* n/a–n/a. doi:10.1002/jps.24535

Malaterre, V., Pedersen, M., Ogorka, J., Gurny, R., Loggia, N., Taday, P.F., 2010. Terahertz pulsed imaging, a novel process analytical tool to investigate the coating characteristics of push-pull osmotic systems. *Eur. J. Pharm. Biopharm.* 74, 21–25. doi:10.1016/j.ejpb.2008.10.011

Mellmann, J., 2001. The transverse motion of solids in rotating cylinders-forms of motion and transition behavior. *Powder Technol.* 118, 251–270. doi:10.1016/S0032-5910(00)00402-2

Mindlin, R.D., 1949. Compliance of elastic bodies in contact. *J. Appl. Mech. ASME* 16, 259–268.

Nase, S.T., Vargas, W.L., Abatan, A.A., McCarthy, J.J., 2001. Discrete characterization tools for

cohesive granular material. *Powder Technol.* 116, 214–223. doi:10.1016/S0032-5910(00)00398-3

Pandey, P., Katakdaunde, M., Turton, R., 2006. Modeling weight variability in a pan coating process using Monte Carlo simulations. *AAPS PharmSciTech* 7, 83. doi:10.1208/pt070483

Pasha, M., Hare, C., Ghadiri, M., Gunadi, A., Piccione, P.M., 2016. Effect of particle shape on flow in discrete element method simulation of a rotary batch seed coater. *Powder Technol.* 296, 29-36.

Pei, C., Wu, C.-Y., Adams, M., 2015. Numerical analysis of contact electrification of non-spherical particles in a rotating drum. *Powder Technol.* 285, 110–122. doi:10.1016/j.powtec.2015.05.050

Pérez-Ramos, J.D., 2007. Monitoring and modeling of film coating in a side vented pan coater using near-infrared reflectance spectroscopy, digital video imaging, and computational methods. PhD Thesis, Purdue University.

Ruotsalainen, M., Heinämäki, J., Guo, H., Laitinen, N., Yliruusi, J., 2003. A novel technique for imaging film coating defects in the film-core interface and surface of coated tablets. *Eur. J. Pharm. Biopharm.* 56, 381–388. doi:10.1016/S0939-6411(03)00118-8

Suzzi, D., Toschkoff, G., Radl, S., Machold, D., Fraser, S.D., Glasser, B.J., Khinast, J.G., 2012. DEM simulation of continuous tablet coating: Effects of tablet shape and fill level on inter-tablet coating variability. *Chem. Eng. Sci.* 69, 107–121. doi:10.1016/j.ces.2011.10.009

Suzzi, D., Radl, S., Khinast, J.G., 2010. Local analysis of the tablet coating process: Impact of operation conditions on film quality. *Chem. Eng. Sci.* 65, 5699–5715. doi:10.1016/j.ces.2010.07.007

Sahni, E., Chaudhuri, B., 2012. Experimental and modeling approaches in characterizing coating uniformity in a pan coater: A literature review. *Pharm. Dev. Technol.* 17, 134–147. doi:10.3109/10837450.2011.649852

Toschkoff, G., Just, S., Funke, A., Djuric, D., Knop, K., Kleinebudde, P., Scharrer, G., Khinast, J.G., 2013. Spray models for discrete element simulations of particle coating processes. *Chem. Eng. Sci.*

101, 603–614. doi:10.1016/j.ces.2013.06.051

Toschkoff, G., Just, S., Knop, K., Kleinebudde, P., Funke, A., Djuric, D., Scharrer, G., Khinast, J.G.,
2015. Modeling of an Active Tablet Coating Process. *J. Pharm. Sci.* 104, 4082–4092.

doi:10.1002/jps.24621

Turton, R., 2008. Challenges in the modeling and prediction of coating of pharmaceutical dosage
forms. *Powder Technol.* 181, 186–194. doi:10.1016/j.powtec.2006.12.006